Journal of Computer-Aided Molecular Design, 2 (1988) 91–106
ESCOM

J-CAMD 037

Computer simulation of the binding of quinocarcin to DNA. Prediction of mode of action and absolute configuration

G. Craig Hill, Timothy P. Wunz and William A. Remers*

Department of Pharmaceutical Sciences, College of Pharmacy, University of Arizona, Tucson, AZ 85721, U.S.A.

Received 9 November 1987
Accepted 20 April 1988

Key words: Molecular mechanics; Computer graphics; Groove binding; Alkylation

SUMMARY

Computer-based models were derived for the covalent and noncovalent binding of the antitumor antibiotic quinocarcin to a representative DNA segment, d(ATGCAT)$_2$. They showed that a mode of action, involving opening of the oxazolidine ring to give an iminium ion, followed by initial noncovalent binding in the minor groove and subsequent alkylation of the 2-amino group of guanine, was rational and attended by favorable interaction energies in each step. The best model had the aryl ring of quinocarcin lying in the 3′ direction from the covalent binding site and an *R* configuration at the carbon involved in covalent bond formation. It also showed that the preferred absolute configuration for quinocarcin was the reverse of that arbitrarily assigned in the literature.

INTRODUCTION

Quinocarcin is an antitumor antibiotic isolated from the culture fluid of *Streptomyces melanovinaceous* [1]. It is a complex pentacyclic alkaloid containing two tertiary amino groups, one of which is protonated at physiological pH (Fig. 1). Ionization of a carboxylic acid group gives it zwitterionic properties [2]. A second compound, quinocarcinol, is elaborated by the same organism. It differs structurally from quinocarcin by not having the oxazolidine ring. Instead, it corresponds to a dihydro-derivative of quinocarcin with the two additional hydrogens on what were C2a and O2 (Fig. 1) [2]. Quinocarcin has been converted into quinocarcinol by sodium borohydride in methanol reduction [2]. The structure of quinocarcinol was established by x-ray diffraction analysis [3]. However, the absolute stereochemistry was not determined. For reasons described below, quinocarcinol and quinocarcin are depicted in Fig. 1 with absolute stereochemistry opposite to that presented in the literature.

*To whom correspondence should be addressed.

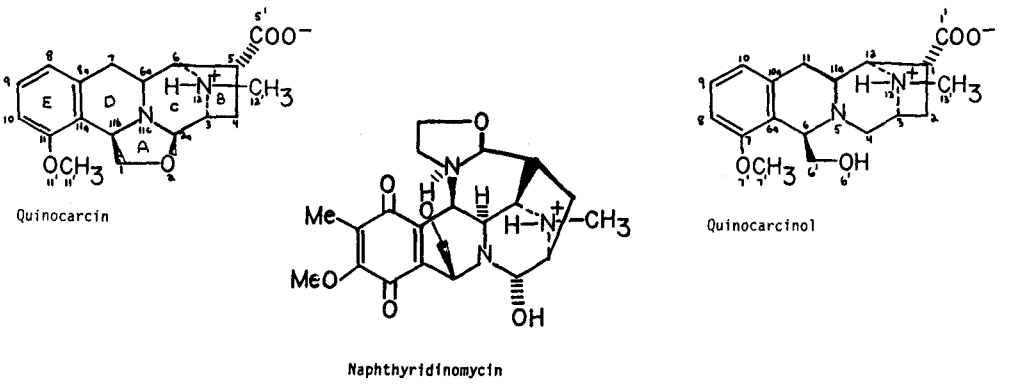

Fig. 1. Structures of quinocarcin, quinocarcinol, and naphthyridinomycin. Each structure is the enantiomer of the one originally proposed in the literature.

Very little information is available on the mode of action of quinocarcin. It is known to block DNA synthesis in preference to RNA and protein synthesis. The cleavage of PM2 covalently closed circular DNA by quinocarcin, but not quinocarcinol, in a reaction stimulated by dithiothreitol and inhibited by free radical scavangers, was reported. [4] However, there is doubt about the importance of this process in living systems because the required concentration of quinocarcin was about 1000-fold higher than those required by typical DNA-cleaving antibiotics including saframycin A and naphthyridinomycin, which have structural resemblances to quinocarcin.

A more plausible mode of action for quinocarcin is alkylation of DNA by opening of the oxazolidine ring, which is related to carbinolamines. This functionality could open to give an iminium ion that would be highly reactive to nucleophilic groups on DNA. Iminium ions have been proposed as the alkylating species for the antitumor antibiotics saframycin A [5,6] and naphthyridinomycin (Fig. 1) [7] and the complementary nucleophilic center on DNA was suggested to be the 2-amino group of a guanine residue. In this case, the drug would make initial noncovalent binding in the minor groove such that its iminium group was close to a guanine residue and then a covalent bond would form. This kind of scenario occurs with the pyrrolo(1,4)benzodiazepines, all of which have a potential iminium forming functionality such as carbinolamine, α-methoxyamine, or imine [8,9]. Saframycins lacking a carbinolamine or equivalent α-cyanoamine functionality cannot alkylate DNA and have no antitumor activity [10]. Quinocarcinol, which lacks the oxazolidine ring of quinocarcin, also fails to affect DNA and it is inactive against tumors and bacteria [1].

Based on the foregoing analysis, we reasoned that modeling of the interaction between quinocarcin and double helical DNA, using the tools of molecular mechanics and computer graphics, might contribute significantly to understanding the mode of quinocarcin's antitumor activity. Of course, computer modeling cannot prove a mode of action. It can, however, give a good indication of how probable a particular mode might be. Thus, if the model for quinocarcin binding shows an obviously good fit to the DNA, a favorable interaction energy, and ease of covalent bond formation, there is a good probability that this could be the mode of action, or one of the modes of action. Subsequent experimental studies could use this model as a starting point for experimental design. In contrast, if a reasonable computer model for DNA binding cannot be developed, experimental studies should be focused in other areas.

One problem in developing a computer model for the DNA binding of quinocarcin is that the absolute stereochemistry has not been established for this molecule. We thought that insight into the stereochemistry might be gained from the computer modeling study. Thus, if both enantiomers of quinocarcin are modeled for binding to DNA, and if the mode of action has a good probability, then there should also be a good probability that the correct enantiomer will bind significantly better than the other enantiomer. There is one previous example of the use of computer modeling to establish the absolute configuration of a molecule. It involved the binding of the antitumor antibiotic CC-1065 to double helical DNA [11]. It is expected, therefore, that the computer model can furnish insight into both the mode of action and the absolute stereochemistry of quinocarcin.

METHODS

Published structures for quinocarcin and quinocarcinol were derived from the crystal structure of quinocarcinol [3]. The structure lacked coordinates for HO6′ (Fig. 1). They were calculated using a bond length of 0.96 Å, a bond angle of 108.5°, and a torsional angle of 180°. The resulting structure was minimized using the program AMBER [12] and all-atom force field parameters presented by Weiner et al. [13]. Some additional parameters, listed in Table 1, had to be defined. The structure of quinocarcin was derived from that of quinocarcinol by removing atoms H4A and HO6′ (Fig. 1), defining a covalent bond between C4 and O6′, and minimizing the energy in AMBER. Enantiomers of the literature structures for quinocarcinol and quinocarcin were obtained by the simple expedient of reversing the sign for each x-coordinate (thus a mirror image). Partial atomic charges (Table 2) were obtained by MNDO calculations [14] using the parameters

TABLE 1
ADDITIONAL BOND, BOND ANGLE AND TORSION ANGLE PARAMETERS NOT GIVEN IN REF. 13

Bond	k_b(kcal/mol Å^2)	R_b(Å)	
CT-NT	367.0	1.47	
CA-OS	450.0	1.38	
Angle	**k_a(kcal/mol rad^2)**	**$a^{(deg)}$**	
CT-CT-NT	80.0	109.7	
CT-NT-CT	70.0	109.5	
CA-CA-OS	85.0	120.0	
NT-CT-CA	80.0	109.7	
CA-OS-CT	100.0	116.3	
NT-CT-OS	80.0	109.7	
HC-CT-NT	35.0	109.5	
Dihedral	**k_d(kcal/mol)**	**(deg)**	***n***
X-CA-OS-X	2.0	0.0	2
X-CT-NT-X	1.0	0.0	6

TABLE 2
ATOMIC CHARGES FOR QUINOCARCIN AND QUINOCARCINOL

Atom[a]	Quinocarcin	Quinocarcinol	Quinocarcinol imminium ion
C1, C6′	0.1697	0.1637	0.1601
H1A, H6′A	0.0285	−0.0243	−0.0118
H1B, H6′B	0.0524	−0.0087	0.0578
O2, O6′	−0.2862	−0.3141	−0.3264
HO6′	-	0.1850	0.2158
C2a, C4	0.2194	0.1617	0.2140
H2a, H4a	−0.0267	0.0367	0.1526
H4B	-	−0.0207	-
C3, C3	0.0101	0.0240	−0.0071
H3, H3	0.0724	0.0560	0.1080
C4, C2	0.0208	0.1617	0.0022
H4A, H2A	0.0609	0.0366	0.0065
H4B, H2B	0.0455	0.0525	0.0934
C5, C1	−0.1392	−0.1341	−0.1255
H5, H1	0.0630	0.0620	0.0722
C5′, C1′	0.3619	0.3616	0.3270
O5′A, O1′A	−0.5724	−0.5661	−0.5316
O5′B, O1′B	−0.5269	−0.5401	−0.5048
C6, C12	0.0399	0.0894	0.0154
H6, H12	0.1035	0.0945	0.1417
C6a, C11a	0.0781	0.1265	0.0632
H6a, H11a	−0.0147	−0.0245	0.0679
C7, C11	0.0594	0.0435	0.0442
H7A, H11A	0.0197	0.0245	0.0679
H7B, H11B	0.0537	0.0613	0.0820
C8a, C10a	−0.0589	−0.0283	−0.0679
C8, C10	−0.0402	−0.0745	−0.0224
H8, H10	0.0729	0.0708	0.0906
C9, C9	−0.0368	0.0111	−0.0010
H9, H9	0.0726	0.0650	0.0944
C10, C8	−0.0529	−0.1336	−0.0347
H10, H8	0.0769	0.0668	0.0978
C11, C7	0.1032	0.1557	0.1226
O11′, O7′	−0.3188	−0.3011	−0.3165
C11′, C7′	0.2033	0.2187	0.1978
H11′A, H7′A	0.0211	0.0941	0.0377
H11′B, H7′B	−0.0196	0.0469	−0.0031
H11′C, H7′C	−0.0305	0.0230	−0.0419
C11a, C6a	−0.0581	−0.199	−0.1412
C11bb, C6	0.0983	0.2167	0.1601
H11b, H6	0.0019	0.0106	0.0562
N11c, N5	−0.3603	−0.4474	−0.1284
N12, N13	−0.0170	−0.0913	−0.0232
HN12, HN13	0.1701	0.1648	0.1835
C12′, C13′	0.1084	0.1183	0.0978
H12′A, H13′A	0.0942	0.0941	0.1054
H12′B, H13′B	0.0536	0.0469	0.0725
H12′C, H13′C	0.0276	0.0230	0.0510

[a]Atoms for quinocarcin are numbered differently than atoms in quinocarcinol and its corresponding iminium ion. In each row, the first entry gives the number of the atom in quinocarcin and the second entry gives the number of the same atom in quinocarcinol or the iminium ion (see Fig. 1).

in MOPAC [15]. The quinocarcinol and quinocarcin structures were then reminimized in AMBER using these charges. A distance-dependent dielectric constant was used and the structure was refined until the rms gradient was less than 0.1 kcal/mol Å. The cutoff distance for non-bonded pairs was 99 Å and the non-bonded pair list was updated every 100 cycles.

Two crucial concerns in using the above models for quinocarcin and quinocarcinol had to be addressed. One was the degree of protonation of the molecules at physiological pH. Our structures, derived from the x-ray analysis of quinocarcinol, have only one of the two basic nitrogens protonated (N12 in quinocarcin). This degree of protonation was chosen for the following reasons: (1) These antibiotics were purified by adsorption onto Diaion WK-20 (H^+ type) resin and then eluted with 2 N ammonium acetate (pH 7.0). Clearly the molecule was not positively charged at pH 7.0, but a neutral zwitterion. No further pH changes were made in converting this eluate into the samples for elemental analysis and x-ray crystallography [2]. (2). A study by Lown et al. showed that saframycin A, which has the same arrangement of basic nitrogens as quinocarcin, was deuterated on only one nitrogen atom, the one corresponding with N12 in quinocarcin, according to its ^{1}H-NMR spectrum in DMSO-d_6/D_2O containing 5% CF_3CO_2D [16]. They suggested that the lone pair on one nitrogen was more accessible than that on the other nitrogen. This same situation should apply to quinocarcin. Furthermore, it must be noted that the proximity of one protonated nitrogen (N12) to the other (N11c) should decrease the pK_a of the second substantially from the expected value of about 10.0. The second concern was stereochemistry at N12 in the models; that is, should the arrangement of the proton and methyl group on this nitrogen be the same as the one found by x-ray analysis or might it be subject to nitrogen inversion in solution or when bound to DNA. Examination of the stereo pair for energy-minimized quinocarcin (Fig. 2) clearly shows that reversing the positions of the proton and the methyl would result in severe steric interaction with H6a. Furthermore, the stereo pairs for the adducts formed between quinocarcin and d(ATGCAT)$_2$ (Figs. 3–7) show in every case that using the x-ray based model results in a structure in which the methyl group points in the direction of the minor groove, whereas in the opposite arrangement it would point into the DNA and cause serious interference with binding. For these reasons, the structures based on the x-ray analysis of quinocarcinol appear to be most appropriate for our study.

Another concern is the configuration of the oxazolidine ring in quinocarcin. Although this does not affect our determination of the covalent binding models from which the absolute configurations of quinocarcin and quinocarcinol were derived, it does affect arguments relating to the mode of action and intermediacy of the iminium ion as depicted in Scheme 1. In the literature, the quinocarcin structure was assigned a *cis*-fused oxazolidine ring on the basis that its ^{1}H-NMR spectrum differed from that of quinocarcinol only by loss of the OH proton and a methine proton at δ 4.95 (J = 3.2 Hz) [2]. It appears to us that this evidence might be consistent with a *trans*-fused

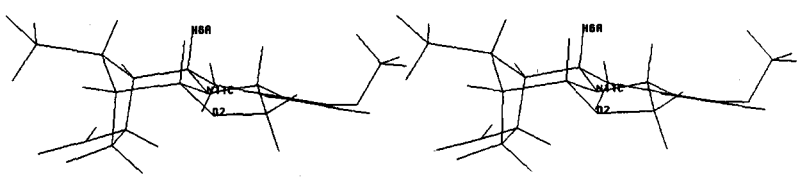

Fig. 2. Stereo pair for quinocarcin.

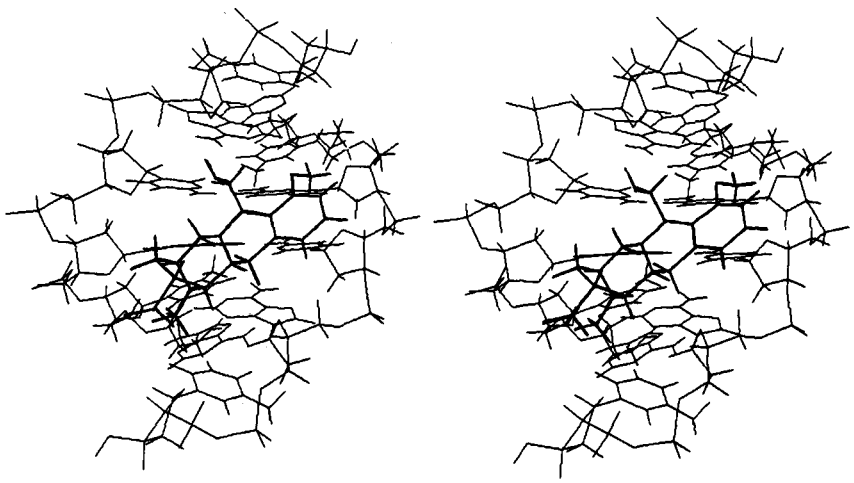

Fig. 3. Stereo pair for covalent quinocarcin with *R* configuration in the 3′ orientation.

oxazolidine ring, which would involve the opposite configuration at C2a. We modeled both of these configurations in order to gain insight into the process of iminium-ion formation.

The minimized drug structures were docked in the appropriate locations and orientations on the hexanucleotide duplex d(ATGCAT)$_2$ with the aid of the interactive graphics program MIDAS [17]. This polynucleotide was constructed in AMBER using Arnott's B-DNA geometry [18] and then minimized. Nomenclature describing it is given in the schematic diagram of Fig. 8. Coordinates of the docked structures were captured and the resulting models were refined by energy minimization using AMBER. The helix distortion energy was determined by subtracting the energy of the helix in a complex from that of the separately minimized isolated helix. Distortion energies induced in the drugs were calculated in the same way.

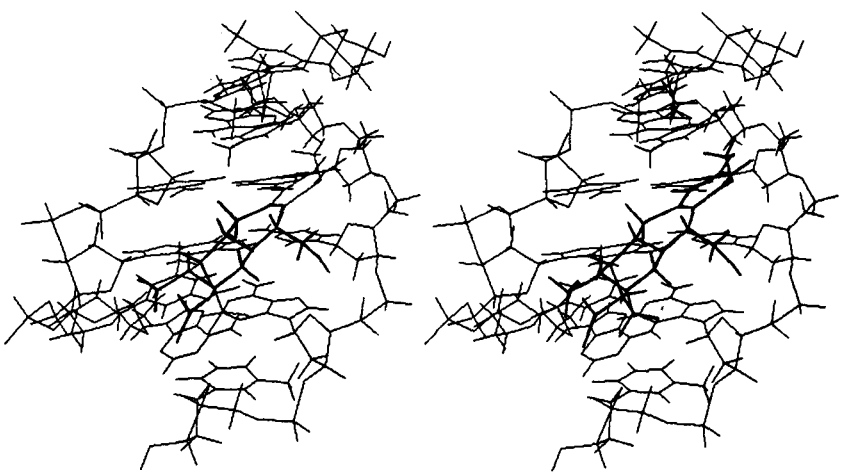

Fig. 4. Stereo pair for covalent isoquinocarcin with *S* configuration in the 3′ orientation.

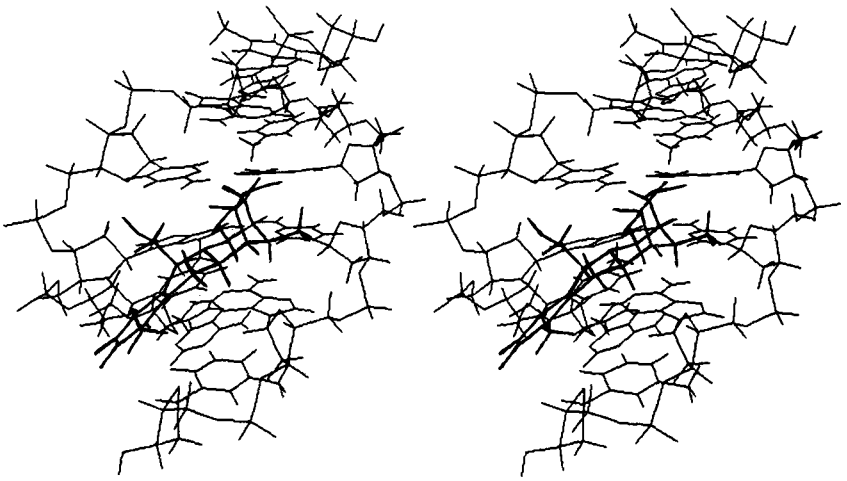

Fig. 5. Stereo pair for covalent isoquinocarcin with *R* configuration in the 5′ orientation.

Two different conformations for the structure of quinocarcin also were modeled. One involved inverting the geometry at N11c so that the lone pair on this nitrogen was *trans* to O2. This transformation was effected by constraining the dihedral angle C7-C8a-C11a-C11b to 44° in the PARM module of AMBER and minimizing the energy. The resulting structure had a boat conformation in ring D and a twist conformation in ring C (Fig. 7), rather than the chair/half-chair conformation shown in Fig. 2. When this structure was reminimized with the constraint removed very little change occurred (the dihedral became 45.7°), showing that it was at a stable local minimum. A similar procedure was used to obtain the conformation with inversion of N11c geometry in the C2a-epimer of quinocarcin.

The effects of solvent and counterions have been neglected in the molecular mechanics calcula-

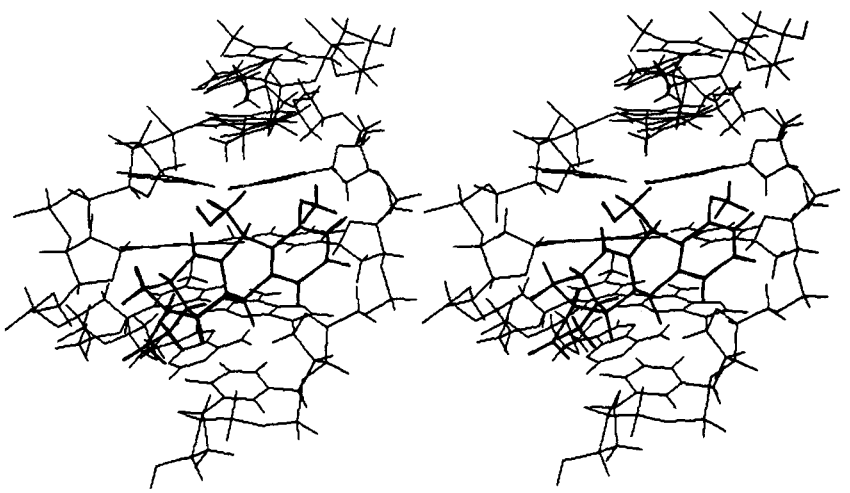

Fig. 6. Stereo pair for the iminium ion noncovalent in the 3′ orientation.

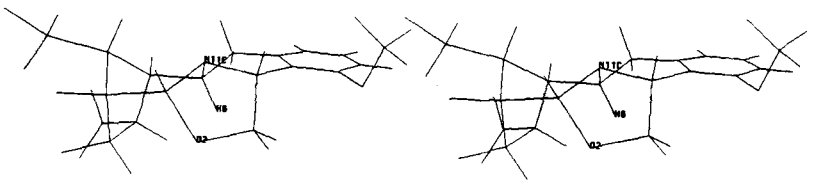

Fig. 7. Stereo pair for quinocarcin in the boat/twist conformation.

tions. However, only small errors should result in the calculated relative net binding energies of various quinocarcin–DNA complexes because they all involve the same drug at the same binding site. Only the orientation and absolute stereochemistry of the drug vary.

RESULTS AND DISCUSSION

In order to determine the best model for the binding of quinocarcin to DNA, we decided to investigate both its covalent and noncovalent binding. The hexanucleotide duplex d(ATGCAT)$_2$ was chosen as a representative segment of DNA. This choice is by necessity somewhat arbitrary, but it is based on the postulation of alkylation at the 2-amino group of guanine and it is the same hexanucleotide that was used for studies on the binding of pyrrolo(1,4)benzodinzepine antitumor antibiotics [19–21]. There are four different orientations in which quinocarcin can bind covalently to guanine in the minor groove of DNA. They involve two different configurations (*R* and *S*) at the carbon atom bound to guanine and two different orientations in the groove. The orientations are denoted 5′ and 3′ depending on which direction the aryl ring lies along the strand containing the covalent binding site. There are also two different enantiomers of quinocarcin to be modeled,

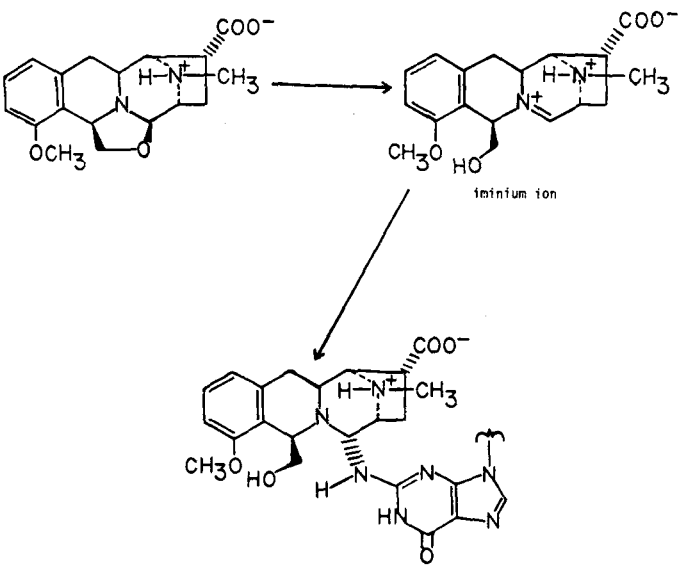

Scheme 1. Proposed mode of action for quinocarcin.

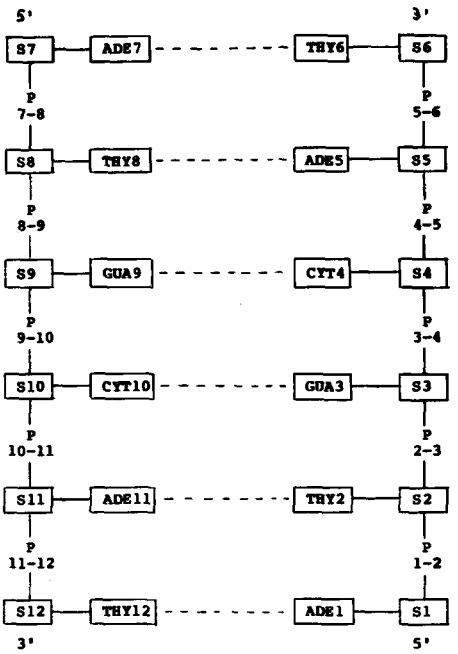

Fig. 8. Schematic for d(ATGCAT)$_2$. S stands for sugar.

which make a total of eight covalent binding models. The quinocarcin enantiomers will be differentiated by calling the one that appeared in the literature isoquinocarcin and the other quinocarcin.

If quinocarcin alkylates DNA, it must undergo opening of the oxazolidine ring with formation of a hydroxymethyl group and a bond between guanine and the carbon that was between the oxazolidine nitrogen and oxygen atoms (Scheme 1). This means that the covalent complex is best constructed in AMBER by starting with quinocarcinol, removing one of the two hydrogens from the carbon atom where the covalent bond will form, removing the appropriate hydrogen from the 2-amino group of guanine, specifying a covalent bond length of 1.47 Å and adjusting the partial atomic charges to reflect the bonding changes. The particular hydrogen atom removed from quinocarcinol determines the configuration in the covalent complex. Performance of these operations, followed by docking of the resulting structures in various orientations on d(ATGCAT)$_2$ and minimization in AMBER, afforded the desired eight models for covalent binding. The relative binding energies of these models are compared in Table 3. In this table, the most important values are the net binding energies, which include the total intermolecular interaction energies minus the energies involved in distortion of the drug and the DNA as they achieve an induced fit in the complexes. The complex with quinocarcin geometry, *R* configuration at the covalent binding site, and aryl ring in the 3′ direction (Fig. 3) is more stable than any other covalent complex by over 8 kcal/mol. Most of this energy difference comes from increased van der Waals interactions. As a group, the complexes derived from quinocarcin are more stable than those derived from isoquinocarcin (-28.8 to -19.1 kcal/mol -21.0 to -5.0 kcal/mol), with the energy differences

TABLE 3
ENERGIES (in kcal/mol) FOR INTERACTIONS BETWEEN QUINOCARCIN SPECIES AND d(ATGCAT)$_2$

Species	Binding mode[a]	Direction and configuration[b]	Total	Intermolecular			Helix distort	Drug distort	Net binding
				vdw	elstat.	total			
Quinocarcin	CV	3′,*R*	−437.9	−24.0	−27.6	−51.6	20.0	2.9	−28.7
	CV	3′,*S*	−428.8	−18.0	−22.2	−39.2	17.1	2.5	−19.6
	CV	5′,*R*	−429.6	−17.8	−25.1	−42.8	18.4	4.0	−20.5
	CV	5′,*S*	−428.2	−20.8	−19.3	−40.0	16.6	4.3	−19.1
Isoquinocarcin	CV	3′,*S*	−430.2	−19.7	−25.6	−45.3	19.6	4.8	−20.9
	CV	3′,*R*	−428.3	−21.7	−19.4	−41.1	15.5	6.6	−19.0
	CV	5′,*S*	−425.4	−20.9	−23.4	−44.2	21.4	6.8	−16.5
	CV	5′,*R*	−414.3	−14.7	−20.9	−35.6	26.5	4.1	−5.0
Quinocarcin iminium ion	NC	3′	−484.6	−27.4	−67.1	−94.5	13.8	2.0	−78.7
Quinocarcin	NC	3′	−429.9	−25.7	−12.4	−38.1	6.9	0.8	−30.4

[a]CV indicates covalently bound and NC indicates noncovalently bound.
[b]Direction refers to the direction that the drug lies in the minor groove and configuration refers to the stereochemistry at C4 in the covalent adducts.

TABLE 4
INTERACTION ENERGIES (in kcal/mol) FOR QUINOCARCIN SPECIES WITH INDIVIDUAL RESIDUES OF d(ATGCAT)$_2$.[a]

Species	Binding mode	Direction and configuration	GUA3	P_{3-4}	CYT4	P_{4-5}	S5	P_{5-6}	CYT10	P_{10-11}	AD E11	P_{11-12}	S12
Quinocarcin	CV	3′,*R*	−12.0						−5.1	−3.1	−5.7		
	CV[c]	3′,*S*	−3.3				−3.2		−3.7	−4.7	−5.0	−4.6	
	CV	5′,*R*	−3.6		−7.7				−4.7		−3.6		
	CV	5′,*S*	−6.7		−3.7	−7.4			−3.3				−4.1
Isoquinocarcin	CV	3′,*R*	−8.2		−3.1	−3.2			−3.6		−3.8		
	CV	3′,*S*	−5.9		−3.1	−4.9					−3.8		
	CV[d]	5′,*R*	−5.5		−4.7		−3.1		−6.4	−4.0			−3.3
	CV	5′,*S*					−3.5	−3.0	−5.0	−6.4	−3.4	−3.8	
Quinocarcin iminium ion[b]	NC	3′	−4.5	−11.1	−6.0	−22.5		−4.5	−4.4	−8.2	−7.9	−9.1	−3.6
Quinocarcin	NC	3′	−3.4								−6.5	−3.2	

[a]Residues are listed only if the energies are ⩾ 3.0 kcal/mol. See Fig. 3 for location of these residues within the DNA.
[b]This species also makes the following interactions: P_{2-3}, −5.5; P_{9-10}, 4.0 kcal/mol.
[c]This species also interacts with S4 by +3.5 kcal/mol.
[d]This species also interacts with S3 by −3.0 kcal/mol.

reflecting van der Waals interactions, helix distortion and drug distortion, all of which are solvent independent parameters.

Table 4 lists energies for the noncovalent interactions of the drug molecules with DNA by individual residues. Those interactions that contribute the most to the binding of the quinocarcin complex with *R* configuration and 3′ direction involve GUA3, CYT10, P_{10-11}, and ADE11 (see Fig. 3 for the DNA schematic). In turn, many of these interactions can be attributed to the formation of specific hydrogen bonds, which are listed in Table 5. It is clear that the complex involving 3′ *R* quinocarcin has a greater network of hydrogen bonds than any other covalent complex. This network involves the proton on O6′ of the drug and O1′ of S5, the proton on N2 of GUA3 and N5 of the drug, a proton on N2 of GUA9 and O7′ of the drug, and a bifurcated system involving the proton on N13 of the drug and N2 of GUA3 and N3 of ADE11. In almost all of the other models there was significant interaction between the drug and N2 of GUA3. The covalent complex with the second best net binding energy involves quinocarcin in the 3′ orientation and *S* configuration at C7 (Fig. 4). Among its interactions with DNA (Table 4) is a strong one with the residue GUA3. In this case, the hydrogen bond forms between HN13 and N3 of the guanine.

The data of Table 3 indicate an overall preference for binding in the 3′ direction. This preference is related to the steric interactions between the methoxyl group of the drug and DNA residues. The methoxyl group can rotate out of the way more easily when it lies in the 3′ direction.

TABLE 5
HYDROGEN-BOND PARAMETERS INVOLVING QUINOCARCIN–POLYNUCLEOTIDE INTERACTIONS[a]

Species	Binding mode	Direction and configuration	Hydrogen atom	Acceptor atom	Length (Å)
Quinocarcin	CV	3′,*R*	HN2 (GUA3)	N5 (QOL)	2.50
			HN13 (QOL)	N2 (GUA3)	2.31
			HN13 (QOL)	N3 (ADE11)	2.45
			HN2 (GUA9)	O7(QOL)	2.26
			HO6′ (QOL)	O1′ (S5)	2.28
	CV	3′,*S*	HO6′ (QOL)	O1′ (S5)	2.27
	CV	5′,*R*	HN13 (QOL)	O2 (CYT4)	2.12
	CV	5′,*S*	HN13 (QOL)	O1′ (S4)	2.48
			HO6′ (QOL)	03′ (P_{11-12})	2.31
Isoquinocarcin	CV	3′,*S*	HN13 (QOL)	N3 (GUA3)	2.16
			HO6″ (QOL)	O1′ (S11)	2.28
			HN2 (GUA9)	O7′ (Q)	2.38
		3′,*R*	HN13 (QOL)	O1′ (S5)	2.24
			HN2 (GUA9)	O7′ (QOL)	2.37
		5′,*S*	HN13 (QOL)	N2 (GUA3)	2.44
		5′,*R*	HN13 (QOL)	O1′ (S11)	2.10
			HO6′ (QOL)	O1′ (S5)	2.16
Quinocarcin iminium ion	NC	3′	HO6′ (QOL)	O (P_{4-5})	1.68
			HN13 (QOL)	N3 (ADE11)	2.29
Quinocarcin	NC	3′	HN2 (GUA3)	O2 (Q)	2.04
			HN12 (Q)	N3 (ADE11)	2.31

[a]QOL indicates numbering as in quinocarcinol (Fig. 1); Q indicates numbering as in quinocarcin.

Except for the 5′ *R* and *S* isoquinocarcin complexes, the DNA helix distortion energies fell into the narrow range of 15.5–20.0 kcal/mol. Conformational analysis of complexes in this range showed that there were no significant changes in the sugar puckers or backbone torsional angles. Instead, the distortion involved many small changes throughout the double helix. No substantial decreases were found in the energies of Watson-Crick base pairing or base stacking. The very poor net binding energy of the 5′ *R* isoquinocarcin complex (−5.0 kcal) resulted partly from a low intermolecular binding, but it also had the highest helix distortion energy. Conformational analysis revealed significant changes in the sugar-phosphate backbone near its point of covalent binding. Thus, the O3′-P-O5′-C5′ and C5′-C4′-C3′-O3′ torsional angles of GUA3 were 158.6° and 90.2°, respectively, compared with 286.2° and 133.6° for the same angles in uncomplexed d(ATGCAT)$_2$. The average phase angle for S4 was 38.0° compared with 93.0° in the uncomplexed DNA and the O5′-C5′-C4′-C3′ torsional angle was 173.1° compared with 63.3°. The stereo pair for this complex (Fig. 5) can be compared with others to get a view of the effects of these distortions. Conformational distortions in the 5′ S isoquinocarcin complex were very similar to those found in the 5′ *R* isoquinocarcin complex, except that the pucker of S4 was more nearly normal.

The foregoing analysis demonstrates that a satisfactory model can be derived for the covalent binding of quinocarcin to a representative DNA segment. Furthermore, it shows that the enantiomer (designated quinocarcin) makes a significantly better model than the structure arbitrarily proposed in the literature. The best binding model has quinocarcin in the 3′ orientation of the minor groove binding with *R* configuration to N2 of guanine. Further support for this model was afforded by studies on the initial noncovalent binding of species that might readily afford the subsequent covalent complex. For this purpose, the iminium ion that would be formed by opening the oxazolidine ring of quinocarcin (Scheme 1) was used to derive a model for the noncovalent complex with d(ATGCAT)$_2$. The resulting complex (Fig. 6) shows an excellent fit between the drug and DNA, with stabilization afforded by a relatively high total intermolecular binding energy of −78.7 kcal/mol (Table 3). Furthermore, C4, which makes the subsequent covalent bond, lies only 3.12 Å from N2 of GUA3. The helix distortion in this complex is only 13.8 kcal/ıol and there are no significant changes from normal in base pairing and base stacking energies, sugar puckers, or backbone dihedrals. Most of the substantial increase in intermolecular binding is electrostatic, probably reflecting the presence of a second cationic center in the intermediate. There are significant interactions between the intermediate and a number of DNA residues (Table 4), but the largest ones are with the negatively charged phosphate groups P_{3-4}, P_{4-5}, P_{10-11}, and P_{11-12}. A short hydrogen bond between HO6′ of the drug and an oxygen of P_{4-5} (Table 5) contributes to the high energy of this interaction. Another important hydrogen bond is formed between the proton on N13 of the drug and N3 of ADE11.

The modeling of an iminium ion as a reactive intermediate in DNA binding implies that it is formed readily from quinocarcin. However, there appears to be a serious problem in using either the literature structure (isoquinocarcin) or our revised quinocarcin structure for generating this intermediate. The problem is that opening of the oxazolidine ring would have to occur in an arrangement in which O2 is in a pseudo-equatorial position and orthogonal to the lone pair of N11c (Fig. 2), a distinctly unfavorable conformation [*]. This problem was examined in two different

*We thank a reviewer for pointing out this crucial consideration and for suggesting that an alternative conformation might solve the problem.

TABLE 6
ENERGIES (in kcal/mol) FOR QUINOCARCIN AND RELATED SPECIES

Species	Calculated energy
Quinocarcin	25.3
Quinocarcin with boat/twist conformation[a]	35.2
C2a-epi quinocarcin	35.4
C2a-epi quinocarcin with boat/twist conformation[a]	32.6

[a]Refers to the conformations in rings D and C.

ways: (1) changing the conformations of the rings containing the nitrogen atoms; and (2) changing the fusion of the oxazolidine ring from *cis* to *trans* by making the epimer at C2a. The latter change is based on a possible ambiguity in the literature structure for quinocarcin, wherein the chirality at C2a was assigned only on the basis of a coupling constant in the ^{1}H-NMR spectrum [2]. As discussed under METHODS, the structure with changed conformation adopts a boat conformation in ring D and a twist conformation in ring C (Fig. 7). It has the favored *trans* coplanar arrangement for the electron pair on N11c and the atoms N11c, C2a, and O2 involved in iminium ion formation. Its calculated energy is higher than that of the unmodified conformation by 9.9 kcal/mol (Table 6). This difference is not much greater than that between the chair and boat conformations of cyclohexane (6.9 kcal/mol), which suggests that the formation of the iminium ion from quinocarcin could occur by way of the boat/twist conformation.

The C2a epimer also was modeled in both the chair/half-chair and twist/boat conformations in rings D and C (Figs. 9 and 10). As shown in Table 6, there is only a relatively small energy difference (2.8 kcal/mol) between these conformations. The twist/boat conformation is the more stable one, which contrasts the results on the quinocarcin conformers. The less stable chair/half-chair

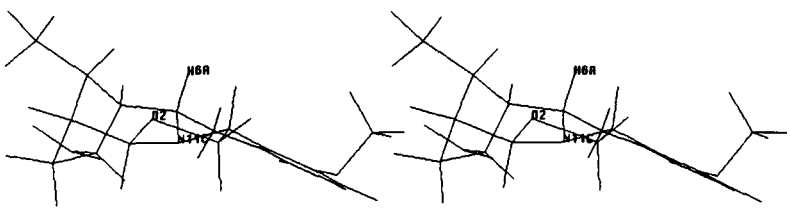

Fig. 9. Stereo pair for C2a-epi quinocarcin.

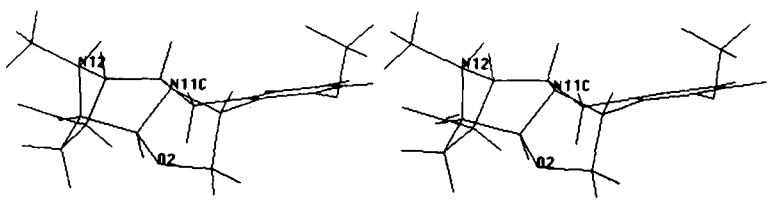

Fig. 10. Stereo pair for C2a-epi quinocarcin in the boat/twist conformation.

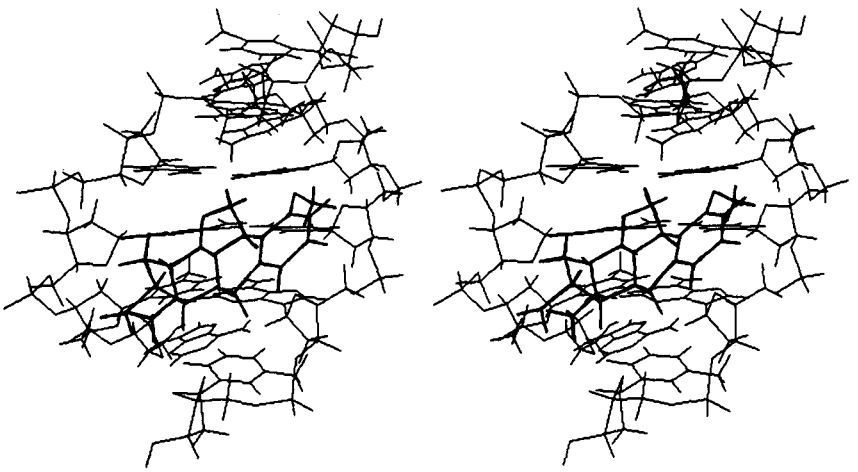

Fig. 11. Stereo pair for quinocarcin noncovalent in the 3′ orientation.

conformation has a *trans* coplanar arrangement of functionalities preferred for iminium ion formation. Based on these results, it appears that iminium ion formation is possible from either quinocarcin or its C2a epimer. There is no way to choose between the two structures with the limited amount of experimental evidence available.

Although the iminium ion complex described above gives an excellent model for initial noncovalent binding, it seemed important to investigate the complex between quinocarcin and d(ATGCAT)$_2$ as a potential model. In principle, quinocarcin could bind near N2 of GUA3 and alkylate it in a process, perhaps concerted, in which the N2 group attacks C2a of quinocarcin as the oxazolidine ring opens. Quinocarcin was docked in the minor groove near N2 of GUA3 and this crude complex was minimized in the usual way. The resulting refined complex (Fig. 11) looked satisfactory and it gave a significant net binding energy (-30.4 kcal/mol) with little distortion of either the helix or the drug (Table 3). However, the distance between the alkylating site of the drug, C2a and N2 of GUA3 is 4.03Å, which is not close enough for subsequent convenient covalent bond formation. Another serious problem with this model is the geometry at the alkylating site of the drug. An attack by N2 of GUA3 with inversion of configuration at C2a simply is not possible because N2 and the oxazolidine oxygen cannot be placed on an axis that goes through C2a. Consequently, this potential model is rejected in favor of the iminium ion model.

CONCLUSIONS

Models for the covalent and noncovalent binding of the antitumor antibiotic quinocarcin to DNA have been derived through the use of molecular mechanics and computer graphics. They feature noncovalent binding of an iminium ion intermediate in the minor groove, with subsequent formation of a covalent bond to N2 of a guanine residue. The preferred alignment in the groove is with the aryl ring of the drug toward the 3′ side of this guanine, and the preferred configuration of the alkylating carbon of the drug is *R*. A better model was obtained when the enantiomer of the structure arbitrarily assigned to quinocarcin was used in the model. These results suggest that it is probable that quinocarcin alkylates DNA in the minor groove to produce its antitumor effect.

This mode of action is closely related to that of naphthyridinomycin (Fig. 1), a drug of similar structure [7]. The absolute stereochemistry of naphthyridinomycin has been revised recently and it corresponds to that of our revised quinocarcin [22]. Although our results do not definitely establish either the mode of action or the absolute stereochemistry of quinocarcin, they provide a rational basis for the design of experimental studies that might decide these questions expeditiously.

ACKNOWLEDGEMENTS

This investigation was supported by NIH National Cancer Institute Grant CA-37798. We thank Professor Peter A. Kollman for helpful advice and for a copy of the program AMBER.

REFERENCES

1 Tomita, F., Takahashi, K. and Shimizu, K., J. Antibiot., 35 (1983) 463–467.
2 Takahashi, K. and Tomita, F., J. Antibiot., 35 (1983) 468–470.
3 Hirayama, N. and Shirahata, K., J. Chem. Soc., Perkin Trans. 2 (1983) 1705–1708.
4 Tomita, F., Takahashi, K. and Tamaoki, T., J. Antibiot., 37 (1984) 1268–1272.
5 Ishigoro, K., Takashashi, K., Yazawa, K., Sakiyama, S. and Arai, T., J. Biol. Chem., 256 (1981) 2162–2167.
6 Lown, I.W., Joshua, A.V. and Lee, J.S., Biochemistry 21 (1982) 419–428.
7 Zmijewski, Jr., M.J., Miller-Hatch, K. and Mikolajczak, M., Chem.-Biol. Interact., 52 (1985) 361–375.
8 Hurley, L.H., J. Antibiot., 30 (1977) 349–369.
9 Thurston, D.E. and Hurley, L.H., Drugs of the Future 8 (1983) 957–971.
10 Kishi, K., Yazawa, K., Takahashi, K., Mikami, Y. and Arai, T., J. antibiot., 37 (1984) 847–852.
11 Reynolds, V.L., Molineaux, I.J., Kaplan, D.J., Swenson, D.H. and Hurley, L.H., Biochemistry, 24 (1985) 6228–6237.
12 Weiner, P.K. and Kollman, P.A., J. Comput. Chem., 2 (1984) 287–303.
13 Weiner, S.J., Kollman, P.A., Case, D., Singh, U.C., Ghio, C., Alagona, G., Profeta Jr., S. and Weiner, P.K., J. Am. Chem. Soc., 106 (1984) 765–784.
14 Dewar, M.J.S. and Thiel, W., J. Am. Chem. Soc., 99 (1977) 4899–4907.
15 Clark, T., A Handbook of Computational Chemistry, Wiley, New York, NY, 1985.
16 Lown, J.W., Joshua, A.V. and Chen, H.-H., Can. J. Chem., 59 (1981) 2945–2952.
17 Langridge, R. and Ferrin, T.E., J. Mol. Graph, 2 (1984) 55–56.
18 Arnott, S., Campbell-Smith, P. and Chandrasekaron, R., In Fasman, G.D. (Ed.) CRC Handbook of Biochemistry, Vol. 2, CRC, Cleveland, OH, 1976 pp. 411–422.
19 Graves, D.E., Pattaroni, C., Krishnan, B.S., Ostrander, J.M., Hurley, L.H. and Krugh, T.R., J. Biol. Chem., 259 (1984) 8202–8209.
20 Cheatham, S., Kook, A., Hurley, L.H., Barkley, M. and Remers, W., J. Med. Chem., in press.
21 Remers, W.A., Mabilia, M. and Hopfinger, A.J., J. Med. Chem. 29 (1986) 2492–2503.
22 Evans, D.A., Illig, C.R. and Saddler, J.C., J. Am. Chem. Soc., 108 (1986) 2478–2479.